Fourier Analyses of Stagger-Period Sequences**

Xubao Zhang*
* Electrical & Electronic Department, Xi'an Electronic Science and Technology University, China;
Research & Development, Unitron (Canada Branch), Sonova, Switzerland. xbzwdl@yahoo.com

Abstract: Stagger-period sequences are a kind of temporal sequences, but Fourier analysis for a uniform-period sequence is not available to a stagger-period sequence; it means that the analytic conclusions would be misleading. We first define essential concepts related to a stagger-period sequence and a stagger-lag autocorrelation matrix, and propose a Fourier transform pair of a stagger-period deterministic sequence and its spectrum; we analyze properties related to this transform pair, such as the orthogonality of a complex exponential sequence, spectral periodic extension, Toeplitz of circularly stagger-lag matrix and the staggered Paseval's theorem, etc.; we verify inverses of each other of this pair, and derives a convergence condition of the transform. Then, another Fourier transform pair of a stagger-lag autocorrelation matrix and its power spectrum density, properties related to this pair, inverses of each other of this pair and a convergence condition of the transform, in this paper, are also studied. During analyzing, the similarities and differences between the uniform-period and stagger-period counterparts are discussed. Two applications of these Fourier analyses, search of optimal stagger periods and spectrum estimation of stagger-period sequences, are also described in details. In the end, the advantages and methodology of this study are summarized.

Key words: stagger-period sequence, staggered Fourier transform pair, staggered power spectrum density, stagger-lag autocorrelation matrix, staggered spectrum estimation

1. Introduction

In the fields of radar transmission, earthquake prediction, radio astronomy and weather forecast, etc., there exists a kind of temporal sequences and spatial signals, which characterize stagger periods and stagger intervals. Because of interferences of turbulence conditions, the astronomical data from Laser-Doppler anemometry may be irregular, reference[1] presented a modified version of the Burg algorithm to make the spectrum estimates more reasonable. Because of influences of geologic structures, the geosensors of earthquake prediction were not located at the uniform intervals[2], the outputs of their sensing system always were nonuniform-interval array signals, the maximum likelihood algorithm was still used but the new test statistic had to be incorporated. The uniform-period transmission of Doppler weather radars causes range-velocity ambiguity, so the stagger-period pulse transmission and multi-PRF have been applied; reference[3,4] developed effective clutter filters which matched the requirements of the staggered transmission of the weather radar. Reference[5] presented a Dirichelet transform pair of nonuniformly sampling signals, but it did not give a proof of inverses of each other. Reference[6] simply proposed a Fourier transform pair of a stagger-period sequence and its spectrum, and introduced its application, but did not prove inverses of each other of the transform pair.

** This project was supported in part by a grand from the National Science Foundation of China, 69172019.

Currently there exists no consistent/integrated Fourier analysis theories to analyze the stagger-period sequences as common uniform-period Fourier analyses do[7,8,9]. In the above projects, most of the researchers adopted the specific theories and different solutions for their own projects, their ideas were to modify signal processing algorithms for uniform-period sequences. In fact, if ones research the relationship between the uniform-period and stagger-period sequences, they probably and easily generalize the uniform-period Fourier analysis to the stagger-period that, and then, some staggered projects may be solved easy as in the uniform-period case. After many years' study on the Fourier analyses of stagger-period sequences, based on the Fourier analyses of the uniform-period sequences, we have created the Fourier transform pair of a staggered deterministic sequence and its spectrum, analyzed the spectral properties, verified the inverses of each other and derived the relationship with its analogue spectrum, etc. Furthermore, by the same method as studying the stagger-period deterministic sequence, we have also created the Fourier transform pair of a stagger-lag autocorrelation matrix and its power spectrum density, and gave the related derivations and discusses. Two effective applications of the stagger-period analysis, search of the optimal stagger periods and spectrum estimation of a stagger-period echo sequence, were introduced in the end. We attempt to integrate the studied results into this paper; the entire analyses we obtained are relatively simple in expressions and much similar to those in the uniform-period Fourier analyses.

2. Essential concepts and properties of stagger-period sequences

If periods $\{T_n\}$ of discrete-time samplings $\{x(t_n)\}$, $n\epsilon\{0,\pm1,\dots\}$ meet

$$T_n \triangleq t_n - t_{n-1} \neq T_{n+1} \triangleq t_{n+1} - t_n \qquad (1)$$

we call the sampling set a stagger-period sequence, briefly a staggered sequence, then $\{T_n\}$ are its stagger periods. If $\{x(t_n)\}$ meets both (1) and

$$T_c = t_{mN_t+l} - t_{(m-1)N_t+l}$$
$$m\epsilon\{0,\pm1,\dots\},\ l\epsilon\{1,2,\dots N_t\} \qquad (2)$$

where T_c is a circular or uniform period of $\{x(t_n)\}$ and equal to $\sum_{i=1}^{N_t} T_i$, N_t is a number of all the mutually unequal stagger periods, we call $\{x(t_n)\}$ a circular stagger-period sequence or circularly staggered sequence. Assume that scale of the stagger periods meets $T_1:T_2:\dots T_{N_t} = K_1:K_2:\dots K_{N_t}$, then the set of the ordered integers $\{K_i\}$ is a stagger code of $\{x(t_n)\}$. If $\{K_i\}$ are mutually prime and meet

$$\tau = T_1/K_1 = T_2/K_2 = \cdots T_{N_t}/K_{N_t} \qquad (3)$$

we call τ the highest common divisor of these periods. Obviously, $\tau = T_c/\sum_{i=1}^{N_t} K_i$,① and an average sampling frequency is $F_a = N_t/T_c$. A circularly staggered sequence with $N_t = 1$ can be considered as a uniform-period sequence. A circularly staggered sequence also is briefly called a staggered sequence. A stagger-period sequence which meets (1) only is a noncircular stagger-period sequence or is considered as a circular stagger-period sequence with $N_t \to \infty$.

Fig.1 shows a circularly staggered sequence $\{x(t_n)\} = sin(2\pi F_0 t_n)$, $n\epsilon\{0,1,\dots,9\}$, $F_0 = 6$Hz, denoted by bar lines. The stagger code, circular period and average sampling frequency are shown in the figure. We can figure out, $N_t = 2$, τ=0.2/7s. The

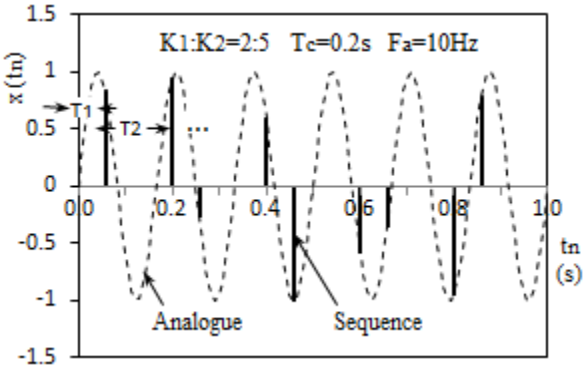

Fig. 1 A stagger-period sinusoid sequence

① Later in this paper, $\sum_{i=1}^{N_t} K_i$ is denoted by $\sum K_i$.

dashed curve is the original analogue signal.

Assume that a stagger-period random sequence $\{x(t_n)\}$, nϵ{0,±1,…} is stationary and meets (1) to (3); conventionally, its autocorrelation matrix is defined as

$$r_x(t_n, t_m) \triangleq E\{x(t_n)x^*(t_m)\} \quad (4)$$

where $E\{\}$ is expectation operator and * is complex conjugation. This equation looks like the auto-correlation matrix of a non-stationary sequence. Even if the staggered sequence is stationary, its auto-correlation matrix does not characterize Toeplitz, i.e.

$$r_x(t_n, t_m) \neq r_x(t_{n+I}, t_{m+I}) \quad n \neq m, \quad I\epsilon\{1,2,\dots N_t - 1\} \quad (5)$$

However, the autocorrelation matrix characterizes Hermitian, i.e. the matrix elements ensure that

$$r_x(t_n, t_m) = r_x^*(t_m, t_n)$$

Furthermore, for a circularly staggered stationary sequence, its autocorrelation matrix has a characteristic of circular Toeplitz, i.e.

$$r_x(t_n, t_m) = r_x(t_{n+N_t}, t_{m+N_t}) \quad n \neq m \quad (6)$$

where N_t is the stagger-period number. Thus, the elements of only one column cannot determine the entire autocorrelation matrix, except the contiguous N_t columns, so many power spectrum analyses of a stationary sequence with uniform periods are not available to the staggered sequences.

3. Fourier analysis of a stagger-period sequence

Lemma: A staggered complex exponential sequence $\{e^{j2\pi f t_n}\}$, $n\epsilon\{0, \pm1, \dots\}$which meets (1) to (3) is normalized, orthogonal in the frequency region $f\epsilon[-B_f/2, B_f/2]$, where $B_f = 1/\tau$, it is referred the spectral period of a stagger-period sequence (proved in the below), specifically,

$$\frac{1}{B_f}\int_{-B_f/2}^{B_f/2} e^{j2\pi f(t_n - t_l)}df = \delta_t(t_n - t_l) \triangleq \begin{cases} 1 & n = l \\ 0 & n \neq l \end{cases} \quad n, l\epsilon\{0, \pm1, \dots\} \quad (7)$$

Proof: If $n=l$, obviously (7) holds. If $n \neq l$, in terms of (1) to (3), we obtain that

$$t_n - t_l = (m\sum K_i + \sum_{j=I_1}^{I_2} K_j)\,\tau \quad \exists\ m\epsilon\{0, \pm1, \dots\}, \exists\ I_1, I_2\epsilon\{1,2, \dots, N_t\} \quad (8)$$

It means that there exists a nonzero integer I which makes $t_n - t_l = I\tau$. Thus,

$$\frac{1}{B_f}\int_{-B_f/2}^{B_f/2} e^{j2\pi f(t_n - t_l)}df = Sinc[\pi B_f(t_n - t_l)] = 0$$

We call (7) the time-domain Dirac function with stagger periods; it shows a similar expression of uniform-period Dirac function (discrete-time sequence) [7].

Assuming that a staggered deterministic sequence $\{x(t_n)\}$, $n\epsilon\{0, \pm1, \dots\}$ meets (1) to (3), we define Fourier transform of this sequence as

$$X_s(f) = \sum_{n=-\infty}^{\infty} x(t_n)e^{-j2\pi f t_n} \quad f\epsilon[-B_f/2, B_f/2] \quad (9)$$

where $B_f = 1/\tau$. We call $X_s(f)$ a staggered Fourier transform of the $\{x(t_n)\}$, or an amplitude spectrum of the sequence, briefly its spectrum. Let $t_l = 0$, from the proof of (7), we know that there exists an integer $I = m\sum K_i + \sum_{j=1}^{I_2} K_j$, m, I_2 are the same as in (8), which makes $t_n = I\tau$, $n\epsilon\{0, \pm1, \dots\}$. Thus,

$$e^{-j2\pi(f+B_f)t_n} = e^{-j2\pi f t_n}e^{-j2\pi I\tau B_f}$$

Since $B_f = 1/\tau$, $e^{-j2\pi I\tau B_f} = 1$. Thus, $X_s(f + B_f) = X_s(f)$ is of a spectral period B_f.

Given Fourier transform (9), we define its inverse Fourier transform as

$$x(t_n) = \frac{1}{B_f}\int_{-B_f/2}^{B_f/2} X_s(f)e^{j2\pi f t_n}df \quad n\epsilon\{0, \pm1, \dots\} \quad (10)$$

and call it a staggered inverse Fourier transform. From (7), we know that the sequence $\{e^{j2\pi f t_n}\}$ is normalized, orthogonal in the frequency region $f\epsilon[-B_f/2, B_f/2]$. This has indicated qualitatively that (10) is validated. In order to ensure that (9) and (10) both form a transform pair, we need to verify their inverses of each other. Inserting (9) into the right-side of (10), we obtain that if (9) is uniformly convergent,

$$\frac{1}{B_f}\int_{-B_f/2}^{B_f/2}\sum_{l=-\infty}^{\infty} x(t_l)e^{-j2\pi f(t_l - t_n)}\,df = \sum_{l=-\infty}^{\infty} x(t_l)\delta_t(t_n - t_l) \quad \text{(in terms of (7))}$$

$= x(t_n)$

Using completely the same way as in uniform period analysis[8], we easily derive that the convergence condition of the Fourier transform (9) are absolutely summable, i.e.

$$\sum_{n=-\infty}^{\infty} |x(t_n)| < \infty \quad (11)$$

This expression is similar to the condition of uniform-period Fourier transform [8].

In practice, the staggered sequences always meet (11), so their spectra exist; theoretically, there is a sequence which does not meet (11), e.g. an impulse train with stagger periods. When we derive the relationship between a spectrum of a staggered sequence and its original analogue spectrum, we need to exploit a technique related to this train. Reference [7] describes a Fourier transform pair of an impulse train and its impulse spectrum with limit convergence operation. Assume that $\tilde{x}(t_n)$ is a stagger-period impulse train which meet (1) to (3), and $x(t)$ is its original analogue signal, then, $\tilde{x}(t_n) = x(t) \sum_{n=-\infty}^{\infty} \delta(t - t_n)$. Without losing generalization, let $t_0 = 0$, and $t_n = mT_c + t_l$, $m \epsilon \{0, \pm 1, \dots\}$, $l \epsilon \{0,1, \dots, N_t - 1\}$, $\tilde{x}(t_n)$ can be denoted by

$$\tilde{x}(t_n) = x(t) \sum_{m=-\infty}^{\infty} \sum_{l=0}^{N_t-1} \delta(t - mT_c - t_l) \quad (12)$$

Let also the spectrum of $x(t)$ be $X^o(f)$, taking continuous-time Fourier transform of both sides of (12) and considering it as a sum of N_t uniform-period trains, we can obtain that the spectrum of $\tilde{x}(t_n)$ [7] ,

$$\tilde{X}_s(f) = \frac{2\pi}{T_c} \int_{-\infty}^{\infty} X^o(g) \sum_{l=0}^{N_t-1} \sum_{m=-\infty}^{\infty} \delta\left(2\pi(f - g + \frac{m}{T_c})\right) e^{-j2\pi(f-g)t_l} dg$$

$$= \frac{1}{T_c} \sum_{m=-\infty}^{\infty} X^o\left(f + \frac{m}{T_c}\right) A(m) \quad (13)$$

where $A(m) = \sum_{l=0}^{N_t-1} e^{j2\pi \frac{m}{T_c} t_l}$ is a modulation sequence. From this Fourier analysis, we conclude that the spectrum of the stagger-period impulse train $\tilde{x}(t_n)$ is composed of a train of the infinite analogue spectra which are displaced at frequency intervals of $1/T_c$, and are individually modulated in amplitude and phase.

In the case of a uniform-period train, its spectrum is composed of infinite replicas of its analogue spectrum, which are displaced at intervals of the sampling frequency F_r[7]. Since these replicas have exactly the same shape as the analogue spectrum, and their phases are unmodulated; it is possible to reconstruct the original analogue signal. However, in the case of a staggered train, its spectrum is composed of the infinite N_t modulated analogue spectra within an average sampling frequency F_a, i.e. N_t times crowding relatively to the uniform-period spectrum, so the spectrum is always in overlapping. Thus it is infeasible to reconstruct the original signal from the staggered spectrum. From the staggered spectrum (13), we can analyze that within one spectral period $B_f = \sum K_i / T_c$, there are $\sum K_i$ spectral lobes with the different shapes to be displaced at the equal interval F_a/N_t. With m=0, the spectral lobe is the highest, called main lobe; the other lobes with $m \neq 0$ are modulated, of lower height, and called fence-lobes.

Fig. 2 shows partial magnitude spectra $|X_s(f)|$ of a staggered sequence $\{Sinc(\pi B_w t_n)\}$, n=1,2,…, in terms of (9), denoted by the dotted and the dashed curves; as well as the spectrum of its analogue signal, $X^o(f)$, denoted by the solid curve,. The spectrum $X^o(f)$ is rectangular, and its bandwidth is B_w=7.5Hz, its spectral center is at 0Hz, and its height is 4. Two spectra of the staggered sequence with two lengths N_p =45 and 9, respectively; average sampling frequency $F_a = 30$ Hz. In the case of N_p=9, these spectral lobes appear off rectangles; in the case of N_p=45, these spectral lobes approach to rectangles. Within a staggered spectral period($B_f = 840\text{Hz}$), there are totally 84 spectral lobes; here only six of them are shown, the two spectral lobes at f =0Hz are the highest. When N_p is increasing, the Gibbs oscillation will tend to disappear, i.e. the spectral jags

of each lobe will be smoothed out.

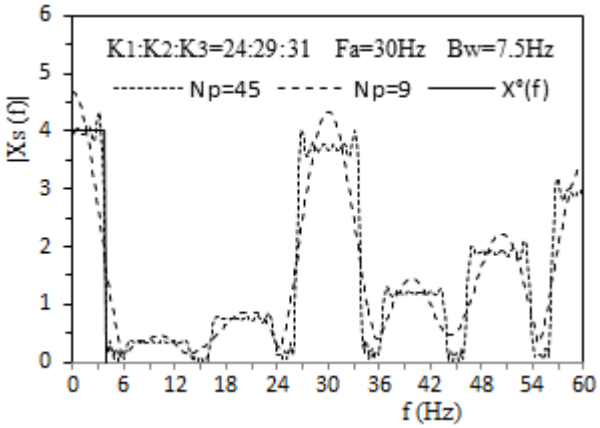

Fig.2 Spectrum of a Sinc sequence with stagger periods

In order to compare the staggered spectra in Fig.2, Fig. 3 shows two magnitude spectra $|X_u(f)|$ of a uniform-period sequence $\{Sinc(\pi B_w nT)\}$, n=1,2,…, in terms of common uniform-period Fourier transform[9], as well as its analogue spectrum $X^o(f)$; the formers are with two lengths N_p =45 and 9, denoted by the dotted and dashed curves, respectively, and the latter, by the solid curve. Well-known, when $N_p \to \infty$, the spectrum $X_u(f)$ involves replicas of its analogue spectrum, displaced at an interval of the sampling frequency F_r=30Hz, each of its repeat spectra have exactly the same shape of

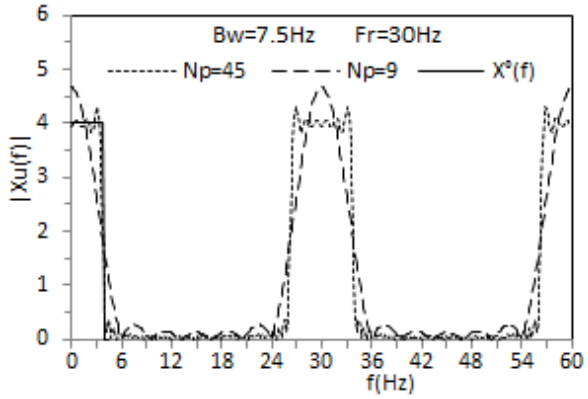

Fig.3 Spectrum of a Sinc sequence with uniform periods

$X^o(f)$, and only one spectrum stands up within one spectral period, i.e. sampling frequency width 30Hz. Thus, we can reconstruct the analogue signal from the uniform-period spectrum.

In fact, the correlations between the staggered samplings change in a little mess from those between uniform-period samplings; the spectrum of the staggered Fourier transform (9) is a little complex but it most validly represents relationship between all the spectral components of a staggered sequence; thus, number of its spectral lobes increase a lot and the complex shapes are reasonable.

Assuming that a staggered deterministic sequence $\{x(t_n)\}$, $n\epsilon\{0,\pm1,\dots\}$, meets (1) to (3), with the transform pair of (9) and (10), we call the following relation,

$$\sum_{n=-\infty}^{\infty}|x(t_n)|^2=\frac{1}{B_f}\int_{-B_f/2}^{B_f/2}|X(f)|^2df \qquad (14)$$

Parseval's theorem of the staggered sequence. The relation is similar to that Parseval's theorem of a uniform-period sequence[9].

Proof: Inserting (9) into the right-side of (14), we can obtain that

$$\frac{1}{B_f}\int_{-B_f/2}^{B_f/2}\sum_{n=-\infty}^{\infty}x(t_n)\sum_{m=-\infty}^{\infty}x^*(t_m)e^{j2\pi f(t_m-t_n)}\,df$$

$$=\sum_{n=-\infty}^{\infty}|x(t_n)|^2 \qquad \text{(in terms of (7))}$$

This theorem indicates that in the case of stagger periods, the total energy of a sequence is equal to the integral of its energy spectrum density within a spectral period. Thus, this relation also makes sense in physics. Reference[10] extended Parseval's relation from uniform-period case to nonuniform-period case, the resulting relation is similar to the uniform-period Parseval's relation too. His definition of the spectrum of a nonuniform-period sequence is complicated, so the proof of the generalized Paseval's relation also is complicated.

4. Fourier analysis of a stagger-lag Autocorrelation matrix

Assuming that a stagger-period stationary sequence $\{x(t_n)\}$, $n\epsilon\{0,\pm1,\dots\}$ meets (1) to (3) and ergodicty, in terms of (4) and (9), we can obtain the

power spectrum density (PSD) of the sequence of length $2N_p+1$,

$$\frac{1}{2N_p+1}E\{|X_{2N_p+1}(f)|^2\}=\frac{1}{2N_p+1}\sum_{n=-N_p}^{N_p}\sum_{m=-N_p}^{N_p} r(t_n,t_m)e^{-j2\pi f(t_n-t_m)} \quad (15)$$

With $N_p\to\infty$, let N_p be integer times of N_t and $t_0=0$, we can denote $m=kN_t+l$, $k\epsilon\{-N_p/N_t,\dots,N_p/N_t\}$, $l\epsilon\{0,\dots,N_t-1\}$. In terms of the circular period of $\{t_n\}$, or the properties of (2) and (6), the right-side of (15) become

$$\frac{1}{2N_p+1}\sum_{n=-N_p}^{N_p}\sum_{k=-N_p/N_t}^{N_p/N_t}\sum_{l=}^{N_t-1} r(t_{n-kN_t},t_l)\, e^{-j2\pi f(t_{n-kN_t}-t_l)}$$

When $N_p\to\infty$, $\{t_{n-kN_t}\}$ is displaced by kT_c along $\{t_n\}$; since $k\epsilon\{-\infty,\dots,\infty\}$, t_{n-kN_t} can be denoted by t_n, $n\epsilon\{-\infty,\dots,\infty\}$. Thus, we define PSD of the $\{x(t_n)\}$ or Fourier transform of its autocorrelation matrix as

$$S_p(f)=\lim_{N_p\to\infty}\frac{2N_p/N_t+1}{2N_p+1}\sum_{n=-N_p}^{N_p}\sum_{l=0}^{N_t-1} r(t_n,t_l)\, e^{-j2\pi f(t_n-t_l)}$$
$$=\frac{1}{N_t}\sum_{n=-\infty}^{\infty}\sum_{l=0}^{N_t-1} r(t_n,t_l)\, e^{-j2\pi f(t_n-t_l)} \quad f\epsilon[-B_f/2,B_f/2] \quad (16)$$

where $B_f=1/\tau$. This definition indicates the relatively powers of different frequency components, and $S_p(f)$ has real, nonnegative values. With the same way as the spectral period of (9) is proved, we can verify that B_f still is the spectral period of the PSD in (16). Because of the circular Toeplitz property (6) of the autocorrelation matrix, the definition (16) using only the N_t column elements is reasonable. Fourier transform of the lth column of the stagger-lag autocorrelation matrix forms a sub-PSD of the column, i.e.

$$S_{pl}(f)=\sum_{n=-\infty}^{\infty} r(t_n,t_l)\, e^{-j2\pi f(t_n-t_l)} \quad l\epsilon\{0,\dots,N_t-1\} \quad (17)$$

This sub-PSD is only based on the $r(t_n,t_l)$ of observation time t_l, and cannot guarantee to be positive values at all the frequencies.

We define the inverse of Fourier transform (16) of a staggered autocorrelation matrix as

$$r(t_n,t_l)=\frac{N_t}{B_f}\int_{-B_f/2}^{B_f/2} S_{pl}(f)e^{j2\pi f(t_n-t_l)}df \quad n\epsilon\{0,\pm1,\dots\},\ l\epsilon\{0,\dots,N_t-1\} \quad (18)$$

where $S_{pl}(f)$ results from (17). We also call (18) spectral decomposition of the stagger-lag auto-correlation matrix. For simplicity, the staggered Fourier transform pair (16) and (18) can have another version,

$$S_p(f)=\sum_{l=0}^{N_t-1} S_{pl}(f)$$
$$=\sum_{l=0}^{N_t-1}\sum_{n=-\infty}^{\infty} r(t_n,t_l)\, e^{-j2\pi f(t_n-t_l)} \quad f\epsilon[-B_f/2,B_f/2] \quad (19)$$

$$r(t_n,t_l)=\frac{1}{B_f}\int_{-B_f/2}^{B_f/2} S_{pl}(f)e^{j2\pi f(t_n-t_l)}df \quad n\epsilon\{0,\pm1,\dots\},\ l\epsilon\{0,\dots,N_t-1\} \quad (20)$$

In the case of a stagger-period sequence, contiguous N_t columns of an autocorrelation matrix involve all information of the matrix, the inverse Fourier transform of the stagger-lag autocorrelation matrix can represent as N_t dimensions. However, in the case of a uniform-period sequence, only one column of an autocorrelation matrix involves all information of the matrix, the Fourier transform pair of the uniform-lag autocorrelation sequence[9] is the special case of (19) and (20) with $N_t=1$. Conventionally, the inverse Fourier transform (20) can be called Weinner-Khimchin equation of the staggered sequence. For validity of the pair (19) and (20), their inverses of each other need to be verified. Inserting the sub-PSD of (17) into the right-side of (20), we obtain that

$$\frac{1}{B_f}\int_{-B_f/2}^{B_f/2}\sum_{k=-\infty}^{\infty} r(t_k,t_l)\, e^{-j2\pi f[(t_k-t_l)-(t_n-t_l)]}df$$
$$=\sum_{k=-\infty}^{\infty} r(t_k,t_l)\,\delta_t(t_n-t_k) \quad \text{(in terms of (7))}$$
$$=r(t_n,t_l)$$

The Fourier transform (19) of the stagger-lag auto-correlation matrix has an expression similar to (9) of the staggered sequence. Thus, the convergence condition of the transform (19) is also absolute summable and easy to be derived, i.e.

$$\sum_{l=1}^{N_t}\sum_{n=-\infty}^{\infty}|r(t_n,t_l)|<\infty \quad (21)$$

This convergence condition is sufficient but not

necessary as that of Fourier transform of uniform-lag auto-correlation sequence[9].

Assume that a triangular autocorrelation matrix with stagger lags, $r(t_n, t_l)$, is

$$r(t_n,t_l)=\begin{cases}1-|t_n-t_l|/T_t & |t_n-t_l|\le T_t\\ 0 & |t_n-t_l|>T_t\end{cases}$$
$$n, l\epsilon\{0,\pm1,\dots\infty\} \qquad (23)$$

where T_t is a half of bottom time width of the triangle. Fig.4 shows the sequence of $r(t_n, t_l)$ with reference time $t_l = 0$, and its parameters: the stagger code, circular period T_c, average sampling frequency

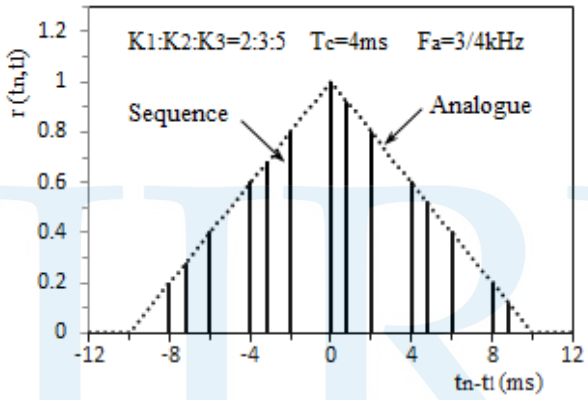

Fig. 4 A stagger-lag triangular autocorrelation sequence

F_a. The dotted curve represents the analogue auto-correlation function; the bar lines represent the stagger-lag autocorrelation sequence.

Fig.5 shows Fourier transform (PSD) of the stagger-lag autocorrelation matrix of (23) $l\epsilon\{0,1,2\}$, with different lengths $N_p = 8$ and 4. Because of circular Toeplitz, the spectral period B_f is 2.5kHz. For each spectrum, there is ten spectral lobes within one B_f: the main lobe is the highest at 0Hz and the other nine fence-lobes are lower, the lowest one is at 1.25kHz. The two PSDs are symmetric about the mid frequency point 1.25kHz. When N_p is enough large to make $r(t_{N_p}, t_l)$ =0, e.g., N_p=8, all values of the PSD $S_p(f)$ are positive reals; otherwise, e.g. when small N_p =4, values of the calculated $S_p(f)$ are negative at some frequencies. In fact, when length of an auto-correlation sequence is cut short enough, the autocorrelation may not represent the auto-correlation of a practical sequence, so negative

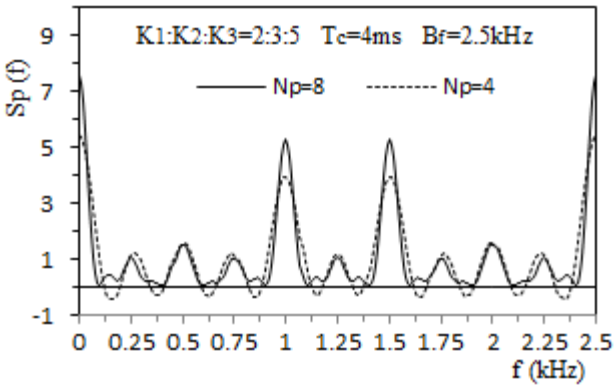

Fig.5 PSDs of a stagger-lag triangular autocorrelation matrix

values of the power spectrum appear at some frequencies. In Fourier analysis of uniform-period sequences, such PSD behaviour also occurs if length of an autocorrelation sequence is incomplete.

Fig.6 shows PSDs of a uniform-lag triangular autocorrelation with different lengths N_p=8 and 4, the autocorrelation sequence is

$$r(nT_r)=\begin{cases}1-|nT_r|/T_t & |nT_r|\le T_t\\ 0 & |nT_r|>T_t\end{cases}$$
$$n\epsilon\{0,\pm1,\dots\pm N_p\} \qquad (24)$$

where T_r is the uniformly sampling period. We selected $T_r = T_c/N_t$ and the analogue autocorrelation function are the same as in Fig.4. in Fig.6, the solid curve represents the PSD of N_p=8, and the dashed curve, N_p=4. In comparison of Fig.5 to Fig.6, we can see that the PSDs of the triangular autocorrelations with stagger lags and uniform lags are close within [-375, 375] Hz, the region is a spectral period of the uniform-lag DSP, the main lobes should be the squared Sinc function if without overlapping; the two spectra may be very different outside [-375,375] Hz, the stagger-lag fence-lobes overlap very much and relatively high; those uniform-lag lobes overlap slightly and almost no fence-lobe with N_p=8, but the repeat spectral lobes are as strong as its main lobe.

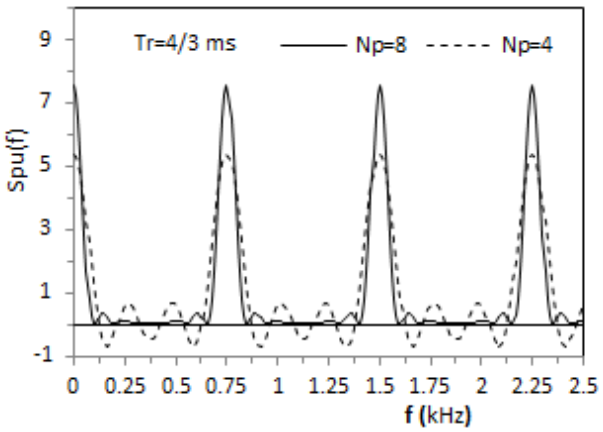

Fig.6 PSDs of a uniform-lag triangular Autocorrelation sequence

5. Applications of stagger-period Fourier analyses

In a modern radars, Doppler frequencies of receiving echoes are very high because the aircraft/target velocity is very high. If we have to select the high PRF(pulse repeat frequency) with uniform-period transmission, the range to observe the targets decrease largely. As pointed out in the section 3, the spectral period B_f of a stagger-period sequence is extended much relatively to the spectrum of a uniform-period sequence. With this principle, stagger-period transmission of a Doppler radar can efficiently eliminate such range-velocity ambiguity. The staggered spectrum estimation (9) is recommended for searching the best stagger periods for the optimal radar target detection.

With the Newman Pearson Criterion, the optimum weights of staggered FIR filters are a solution of a linear system of the complex equations. Assume that filter weights are $\{h_l(t_n)\}$, n=1,…, N_s, N_s is a number of coherent echo samplings, l=1,…, N_w, N_w is a number of filters in a bank. At first, we need a given staggered covariance matrix of the clutters plus noise and a given staggered target signal vector which is averages of an aircraft echoes over all Doppler frequencies; they should be prior knowledge. This algorithm is called the Match Algorithm which enable the S/N improvement factor to be maximum, as that factor obtained with the uniform PRF optimal algorithm. After a pulse train is filtered for N_w sliding windows, outputs of these filters are summed and the filtering system forms a relatively flat frequency response over the Doppler frequency region. This response is called a velocity response of the staggered MTI (moving target indicator) filters. It can be calculated by

$$V_s(f)=\frac{1}{N_w}\sum_{l=1}^{N_w}|H_i(f)|$$

where $H_i(f)$ is the frequency response of the lth MTI filter, f is Doppler frequency of a target; $H_i(f)$ can be calculated in terms of (9), replacing $x(t_n)$ with $h_l(t_n)$. For the optimal Doppler target detection, $V_s(f)$ is requested to be a flat response. So nonflatness of the velocity response is defined as

$$D_v=\max_{f\epsilon B_p}\{V_s(f)\}-\min_{f\epsilon B_p}\{V_s(f)\}$$

where B_p is passband region of the velocity response as the staggered spectral period B_f described in the section 3. Different stagger codes $\{K_1:K_2:\dots K_{N_s}\}$ result in different $\{H_i(f)\}$ and different $\{D_v\}$. The less the D_v, the flatter the $V_s(f)$. The optimal stagger code can be solved with the following discrete nonlinear mathematical programming

$$\begin{cases}\min D_v(K_1:K_2:\dots K_{N_s})\\ K_1,K_2,\dots K_{N_s}\ prime\ to\ each\ other\\ \max_j\{K_j\}/\min_j\{K_j\}\le R_t\\ \frac{1}{N_s}\sum_{i=1}^{N_s}K_i>R_f\end{cases} \quad (25)$$

where R_t is a given stagger ratio, and R_f is a given extension factor of blind speed, equal to a ratio of the staggered spectral period to the uniformed spectral period, see the section 3. When several heuristic strategies are incorporated, the mathematical programming can be efficiently solved. For example, the search frequency region B_p is not selected as the entire staggered spectral period, but rather a part of the period, i.e. where the Doppler targets often happen, we call the frequency region the passband

region B_p . Based on spectral parameters of the terrain clutter: power, center and bandwidth, we selected the common clutter spectral model, Gaussian spectrum[11], and calculated out N_w optimum filters, then the stagger code can be searched out with (25).

Fig.7 shows velocity responses of two banks of MTI filters with the same R_t(1.2) and very close R_f (27.6 and 27.4) and two searched stagger codes. The two sets of MTI filtering weights match different stagger codes respectively and both are optimum to suppress the given terrain clutter; but the nonflatness of their velocity responses are much different: D_v with the stagger code (25,29,26, 28,30) is 16.3 dB, the best code, and D_v with the stagger code (25,26,29,30,27) is 25.7 dB, the worst code. After obtained the best code and given average sampling frequency, following the section 2, we can calculate the best corresponding stagger periods.

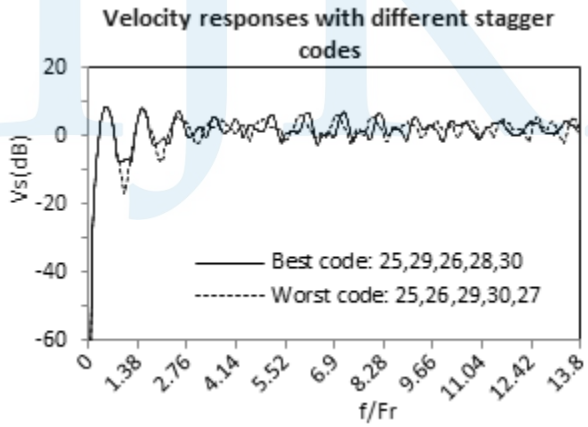

Fig.7 Comparison of the best to the worst velocity responses

Another application of the stagger-period Fourier analysis is regarding spectrum estimation. Reference[12] proposed a uniform-period method of autocorrelation spectral density to produce the unbiased estimates with phase information, and was going to start the same estimation under the stagger-period condition. Here one of our great examples is a staggered LP(linear prediction) spectrum estimation. Given that $\hat{r}(t_n, t_l)$ is an autocorrelation matrix estimate of a circularly staggered stationary sequence; we selected the sampling number $N_p = 5$, the stagger code is (25,29,26,28,30) and average sampling frequency $F_a = 360$Hz; with (1) to (3), we calculated out that the corresponding stagger periods are [2.516, 2.919, 2.617, 2.818, 3.019] ms. Furthermore, assume that $\{\hat{h}(t_n)\}$, $n\epsilon\{1,2,\dots N_p - 1\}$ are estimates of one-step backward prediction coefficients of the sequence, then $\{\hat{h}(t_n)\}$ are solved by the following Yule-Walker equation with stagger periods,

$$\sum_{n=1}^{N_p-1} \hat{h}(t_n)\,\hat{r}(t_l, t_n) = \hat{r}(t_l, t_0) \quad l\epsilon\{1,2,\dots N_p - 1\}$$

The staggered LP spectrum estimate at observation time t_0 is defined as

$$S_{LP}(f, t_0) = \frac{\sigma(t_0)}{2\pi\left|1+\sum_{n=1}^{Np-1} \hat{h}(t_n)\exp[-j2\pi f(t_n - t_0)]\right|^2} \quad (26)$$

where $\sigma(t_0)$ is the prediction error power at time t_0. The LP estimation is a nonlinear and parametric method. In order to evaluate the performance, we also calculated spectral estimates of the same clutter echoes with uniform periods, which use the average sampling period 2.778 ms as the uniformly sampling period.

Fig.8 shows two spectra of the stagger-period and the uniform-period LP estimations, as well as the spectrum of the tested analogue process. The dashed curve represents the stagger-period estimates, and the dotted curve, the uniform-period estimates, and the solid curve, spectrum of the tested analogue process,. The analogue process was selected as a bimodal Gaussian clutter echo[11], which involves a terrain clutter and a weather clutter; the former's parameters are power/noise=60dB, spectral center=72Hz and standard variance=7.2Hz, and the latter's parameters are power/noise=40dB, spectral center=144Hz and standard variance=14.4Hz. In Fig.8, the X axis represents the normalized frequency f/F_r F_r is the uniformly sampling frequency, it was selected to be equal to the average sampling

frequency F_a of the staggered echoes; the Y axis represents the normalized power spectrum,

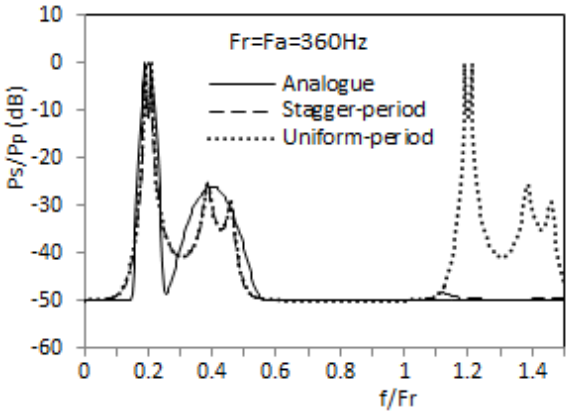

Fig.8 Comparison of a stagger-period to uniform-period spectrum estimations

$S_{LP}(f,t_0)/P_p$, P_p is the maximum of $S_{LP}(f,t_0)$. We can see that the estimates with the stagger periods and uniform periods are almost the same within region 0~F_r, the fitness of the two estimations to the analogue spectrum is good although these estimated lobes show the split peaks; however, the stagger-period estimates are completely different from the uniform-period those with f>F_r, the uniform-period estimation shows a spectral replica in every F_r region but the stagger-period estimation does not. The stagger-period estimation behaves with a great advantage: it is able to restrain ambiguity of repeat spectra caused by the uniform-period estimation. Additionally, this staggered estimation behaves with close spectrum fitness, high bimodal resolution with a short sequence(N_p=5); but it shows possible peak-bias due to spectrum split, and large computation load and word length are required. The stagger-period estimation is applicable to spectrum estimations which require high resolution, especially to off-line spectral analysis.

Based on the staggered Furious analyses in this paper, we are going to study stagger-period, optimal FIR, IIR and lattice filters, and to enable them to behave as under the uniform-period condition.

6. Summarization

This paper has comprehensively described the Fourier analyses for the staggered sequences and the staggered autocorrelation matrixes. The creative work is based on the successes of the existing Fourier analyses for uniform-period sequences. The main work of this paper is the proposed two Fourier transform pairs for both the stagger-period sequence and the stagger-lag autocorrelation matrix, and the verified inverses of each other. At first, this paper defines the new concepts related to the transform pairs, such as the time-domain orthogonality of the staggered complex exponential sequence and the Toeplitz property of the circularly staggered auto-correlation matrix, etc. In the case of a uniform-period sequence, its spectrum and PSD are exactly the same as those of its original analogue signal respectively so long as the spectral overlap does not occur. Unlike the spectrum of a uniform-period sequence, the stagger-period spectrum forms modulated-differently spectral lobes; the number of these lobes increases by N_t multiples within an average sampling frequency, i.e. N_t times crowding relatively to the uniform-period spectrum; so these spectral lobes always overlap. The more the staggered period number of a sequence, the wider its extended spectral period, than the uniform-period case. This property does not make sense for restoring the original signal from the staggered spectrum; however, the staggered Fourier analysis expressions truly represent relationship between all the spectral components of a staggered sequence because the sampling periods in the analytic expressions match the irregularly staggered periods of a sequence. Furthermore, based on this paper's analyses, the staggered spectrum shows a great effect of periodic extension, $\sum K_i/N_t$ multiples of the average sampling frequency, so it is helpful to eliminate the range-velocity ambiguity of a Doppler radar echoes and to restrain the spectrum repeat of the

uniform-period spectrum estimation.

These expressions of Fourier analyses are relatively simple and similar to those counterparts of uniform-period analyses. This is a major difference between our results and the other paper's results. The methodology of this unique study is 1) to convert general stagger periods of a sequence into circularly stagger periods; 2) to use the uniform-period theories for creating Fourier analyses of the circularly staggered sequences, in the case of N_t =1, the expressions of the staggered Fourier analyses in this paper are the same as those with uniform periods; 3) to make the highest common divisor of the stagger periods for simplifying analytic expressions; 4) to properly select the number of the stagger periods and stagger code so that the analyses can be used for various, specific practices. These staggered analytic expressions are relatively simple and consistent with those common uniform-period expressions. Although the analyses in this paper requires the stagger code to meet (2) and (3), we can find such a code or an approximate code in practical applications.

The future work on the Fourier analysis with stagger periods can be their practical applications in signal processing systems, such as implemented structures of the FIR and IIR and lattice filtering for the stagger-period sequences, the spectrum estimation with stagger periods, and their performance evaluations.

Acknowledgments: I would like to thank Prof. Xueyu Peng for his support and encouragement during applying for this project funding. I also thank Prof. Zeng Bao for his directing this study.

References

[1] Robert Bos, Stijn de Waele, Piet M. T. Broersen, Autoregressive spectral estimation by application of the Burg algorithm to irregularly sampled data, IEEE Trans. Instrumentation and measurement, vol. 51. no. 6, Dec. 2002, pp. 1289-1294.

[2] David R. Brillinger, A maximum likelihood approach to frequency-wavenumber analysis, IEEE Trans. ASSP, vol. 33. no. 4, Oct. 1985, pp.1076-1085.

[3] Dmitri N. Moisseev, Cuong M. Nguyen, V. Chandrasekar, Clutter suppression for staggered PRT waveforms, J. Atmos. Oceanic Technol. vol. 25. Dec. 2008, pp.2209-2218.

[4] John Y. N. Cho, Edward S. Chornoboy, Multi-PRI signal processing for the terminal Doppler weather radar. Part I: Clutter filtering, J. Atmos. Oceanic Technol. vol. 22. May 2005, pp.575-582.

[5] Andrzej Wojtkiewicz, Michal Tuszynski, Application of Dirichlet transform in analysis of nonuniformly sampling signals, in Proc. ICASSP. 1992, pp.v25-v28.

[6] Laiyao Fan, Xubao Zhang, Hongbing Ji, A study of Fourier analysis for staggered sampling sequences, ACTA Electronica Sinica, vol.22, no.7, 1994, pp.76-83.

[7] Athanasios Papoulis, Signal Analysis, New York McGraw-Hill Book Company, New York, 1977.

[8] John G. Proakis, Dimitris. G. Manolakis, Digital Signal Processing-Principles, Algorithms, and Applications, 3rd ed. Prentice-Hall Upper Saddle River, New Jersey, 1996. pp.256-259.

[9] Alan V. Oppenheim, Ronald W. Schafer, John R. Buck, Discrete-Time Signal Processing, 2nd ed. Prentice-Hall Upper Saddle Inc. New Jersey, 1999.

[10] A. Luthra, Extension of Parseval's relation to nonuniform sampling, IEEE Trans. ASSP. vol.36, no.12, Dec. 1988, pp.1909-1911.

[11] Brian J. Jackel, Characterization of auroral radar power spectra and autocorrelation functions,

Radio Science, vol.35, no.4, Jul-Aug 2000, pp.1009-1023.

[12] David A. Warde, Sebastian M. Torres, The autocorrelation spectral density for Doppler-weather-radar signal analysis, IEEE Trans. Geoscience and Remote Sensing. vol.52, no.1, 2014, pp.508-518.

Xubao Zhang received the M.S. degree in electronic engineering from Nanjing Aeronautical Institute, Nanjing, China, in 1982, and Ph. D. degree in electronic engineering from Xi'an Electronic Science and Technology University, Xi'an, China, in 1990. He was a post-doctoral Fellow at McMaster University, Hamilton, Canada, in 1993 and 1994.

From 1983 to 1993, he was a lecturer and an associate professor with Xi'an Electronic Science and Technology University, China; he studied DSP for radar, and focused on stagger-period DSP. From 1993 to 1994, he was a research scientist and studied DSP for communication with McMaster University, Hamilton, Canada. Since 1997, he had been a Canadian. As an electronic engineer, he did research and development on signal processing for hearing instruments with Unitron (Canada Branch), Sonova, Switzerland. Now, his continuous interests are on spectral analysis and digital filtering of stagger-period sequences, as well as hearing DSP. He is the author of one book and over 40 articles.

He was awarded the second-prize of Science and Technology Progress by National Science & Technology Committee of China in 1989, and received several Excellent Paper Awards during his university's work in China.